Theoretical Comparative Study of Free Base Porphyrin, Chlorin, Bacteriochlorin, and Isobacteriochlorin: Evaluation of the Potential Roles of *ab Initio* Hartree−Fock and Density Functional Theories in Hydroporphyrin Chemistry

Abhik Ghosh

Department of Chemistry, Institute of Mathematical and Physical Sciences (IMR), University of Tromsø, N-9037 Tromsø, Norway

Received: December 13, 1996[⊗]

Local density functional (LDF) and *ab initio* Hartree-Fock (HF) calculations are reported for free base porphyrin, chlorin, bacteriochlorin, and isobacteriochlorin. The LDF optimized geometries provide a detailed picture of the structural effects of peripheral hydrogenation on the $C_\alpha-C_\beta$ and $C_\beta-C_\beta$ bond distances, the $C_\alpha-C_\beta-C_\beta$ and $C_\alpha-N-C_\alpha$ angles, and the size of the central metal-binding cavity of the macrocycles. The optimized structures of the isobacteriochlorin tautomers are of particular interest. The structure of the *cis* tautomer bears a close resemblance to *cis*-porphyrin, an intermediate in the double-proton migration of free base porphyrins. Since the minimum-energy points of tetrapyrrole potential energy surfaces at the HF level correspond to unrealistic frozen resonance forms with alternating single and double bonds, the delocalized LDF optimized geometry of the low-symmetry *trans*-isobacteriochlorin provides a good example of the advantages of density functional theory (DFT) over HF theory in tetrapyrrole geometry optimizations. The latter structure also provides a good illustration of the structural effects of $C_\beta-C_\beta$ hydrogenation, especially on the $C_\alpha-N-C_\alpha$ angles. The LDF valence ionization potentials (IPs) of the hydroporphyrins, whose absolute values are expected to be in near-quantitative agreement with true experimental values, can serve as a valuable substitute for nonexistent photoelectron spectroscopic data. The lowest LDF and HF IPs of the tetrapyrroles, which decrease with increasing peripheral saturation, correlate well with electrochemical data. LDF calculations on cationic states of different symmetries indicate that the two lowest IPs of hydroporphyrins should lie within approximately 0.5 eV of each other and the third IP should exceed the second by 1 eV or more. Thus, the four-orbital model of porphyrin electronic structure applies reasonably well to hydroporphyrin IPs and photoelectron spectra. LDF equivalent-core calculations provide a detailed picture of molecular charge distributions of hydroporphyrins, key aspects of which are in excellent agreement with available X-ray photoelectron spectroscopic (XPS) data. In contrast, HF theory, which has provided a good description of the XPS of a number of porphyrinic molecules, yields rather poor molecular charge distributions for hydroporphyrins. Overall, in quantitative studies of both structural and electronic properties of hydroporphyrins, HF theory performs rather poorly or even unacceptably. In contrast, the performance of DFT was excellent in every way.

I. Introduction

A wide variety of tetrapyrroles are distributed in nature, including porphyrins, chlorins, bacteriochlorins, isobacteriochlorins, oxygenated hydroporphyrins, and tetrapyrroles with interrupted conjugation.[1] In spite of their broad structural similarity, there are major electronic differences among these ring systems in properties such as light absorption characteristics, redox potentials, metal ion affinities, reactivity of the bound metal toward axial ligands, conformational flexibility, etc. It is widely expected that a detailed characterization of this electronic diversity will also bring about a better understanding of the chemical basis of their diverse biochemical roles. Thus, much effort has been devoted to physical measurements and theoretical modeling[2] of the electronic differences among different tetrapyrroles. The theoretical work has furnished many significant insights, but the methods used, chiefly semiempirical quantum chemical techniques, are modest by today's standards. This motivated us to undertake an initial evaluation of the potentially important role that modern first-principles methods can play in this exciting area.

Given the general lack of first-principles calculations on hydroporphyrins,[3] our first goal was to characterize the performance of some of the more practical first-principles methods in studies of molecular structures, thermodynamic stabilities, and electronic properties of hydroporphyrins. Accordingly, we carried out *ab initio* Hartree−Fock (HF), density functional theoretical (DFT), and (in one case) second-order Møller−Plesset perturbation theory (MP2) calculations on the parent free base tetrapyrroles, namely, free base porphyrin,[4] chlorin, bacteriochlorin, and the *cis* and *trans* tautomers of isobacteriochlorin (Figure 1). A comparison is presented of the quality of the local density functional (LDF) and HF results, which should furnish useful guidelines for future theoretical research on hydroporphyrins.

The calculations also afford a variety of chemical insights.

The optimized LDF structural data, besides being in generally excellent agreement with crystallographic data, also complement experimental information. Thus, the structure of *cis*-isobacteriochlorin reveals a remarkably distorted tetrapyrrole core, which has so far not been observed experimentally. The structure of *trans*-isobacteriochlorin offers a uniquely detailed view of the structural effects of peripheral hydrogenation.

Another significant contribution of this work is the collection of LDF valence ionization potentials. Experimental valence photoelectron spectra, which would allow a definitive and

[⊗] Abstract published in *Advance ACS Abstracts,* March 15, 1997.

S1089-5647(96)04069-2 CCC: $14.00

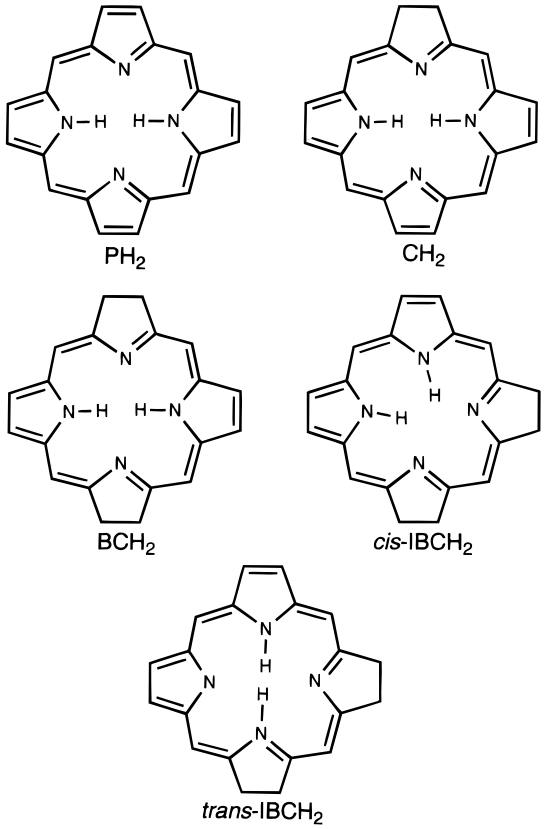

Figure 1. Molecules studied in this investigation.

detailed understanding of the electronic effects of peripheral hydrogenation of porphyrin, are almost nonexistent for hydroporphyrins. Therefore, our LDF valence IPs, which are believed to be extremely accurate, constitute a unique surrogate for the experimental spectra.

Finally, DFT equivalent-core and HF calculations are used to simulate the nitrogen core X-ray photoelectron spectra of hydroporphyrins. The results provide an insightful picture of molecular charge distributions of hydroporphyrins.

This work represents the first major DFT investigation of hydroporphyrins.[3] The results provide a unique sampling of the quantitative structural and electronic data that DFT can readily provide on this class of molecules.

II. Methods

We have previously shown that HF theory is generally unsuitable for geometry optimizations of tetrapyrroles.[3] The minima of HF potential energy surfaces of tetrapyrroles correspond to frozen resonance forms with alternating single and double bonds rather than realistic delocalized structures.[3] The problem is solved by use of correlated methods such as second-order Møller−Plesset perturbation theory (MP2) or DFT.[3] As a good compromise between quality of the results and affordability, we have chosen to use LDF theory for all geometry optimizations.[5] Specifically, we have used the local exchange-correlation potential due to Hedin and von Barth,[6] numerical double-ζ basis sets ("DNP"), and a very fine mesh for numerical integrations, as implemented in the DMol program system.[7] Being confident that symmetry constraints at this level of theory merely save computation time but introduce no artifacts in the results, we optimized PH_2, CH_2, BCH_2, *cis*-$IBCH_2$, and *trans*-$IBCH_2$ (Figure 1) using D_{2h}, C_{2v}, D_{2h}, C_{2v}, and C_s symmetry constraints, respectively. In addition, we also optimized *meso*-tetraphenylporphyrin ($TPPH_2$) and *meso*-tetraphenylbacteriochlorin ($TPBCH_2$) with D_{2h} constraints and with the phenyl groups held perpendicular to the mean tetrapyrrole planes.

Ab initio spin-restricted HF calculations were performed on the LDF optimized geometries using the same symmetry constraints, generally contracted double-ζ (DZ) basis sets,[8] and the direct SCF program DISCO.[9] The calculated core and valence ionization potentials (IPs) that are obtained from HF calculations are simply sign-reversed orbital energies, i.e. obtained by Koopmans' theorem (KT). Basis set effects are not discussed in this study, since our previous work on porphyrins[4a,10,11] suggests that our HF/DZ orbital energies should be essentially converged to the HF limit.

LDF valence IPs were obtained by a ΔSCF procedure.[4b,12,13] In more detail, the total energy of a neutral molecule was subtracted from the total energies of cationic doublet states of different symmetries, spin-unrestricted LDF calculations being performed for both the neutral and cationic states. Since a many-electron wavefunction does not exist in the LDF formalism, one cannot impose orthogonality constraints between different states. Accordingly, the method inherently lacks the ability to describe excited states except in cases where such orthogonality to all lower states is ensured on symmetry grounds. Therefore, it was only possible to calculate the energetically lowest state for any particular symmetry species of the tetrapyrrole cations.

Calculated core IPs provide experimentally testable descriptions of molecular charge distributions. At present, explicit first-principles calculations of core-ionized states of large molecules such as porphyrinoids are impractical. However, in contrast to absolute values, *shifts* in core IPs due to differences in chemical environment can be estimated relatively simply. For instance, shifts in HF-KT core IPs often compare quite favorably with X-ray photoelectron spectroscopic (XPS) data.[9,14] However, HF-KT IPs incorporate neither orbital relaxation effects nor any correlation effects, and we have uncovered cases[11,15] among porphyrinic systems for which HF theory provides an inadequate description of molecular charge distributions and core IPs.

Accordingly, we examined another approach here (henceforth called LDF-EC), namely LDF calculations in conjunction with the equivalent-core (EC) or $Z+1$ approximation.[16,17] The basic idea of the EC approximation is that on ionization of a K-shell electron, the valence electrons relax as if the nuclear charge had increased by one unit. Using this approximation, we represent a nitrogen core ionized state by replacing the nitrogen with an oxygen (i.e. increasing the nuclear charge by one and using an oxygen basis set), keeping the molecular geometry and number of electrons the same as in the un-ionized state, and converging a (spin-restricted, in our case) ground-state closed-shell LDF calculation on the oxaporphyrin molecular cation. The vertical LDF-EC "IP" is then simply the energy difference between the ground states of unionized porphyrin and the corresponding oxaporphyrin cation. The absolute values of HF-KT or LDF-EC "IP" deviate from experimental values by large margins, but the deviations may be regarded as simply systematic errors. In general, for a particular element, trends in EC-based "IPs" closely parallel the trends observed experimentally by XPS. To facilitate a comparison of the HF-KT and EC "IPs", we will cite all IPs relative to a common zero level, namely, the core IP of the unprotonated nitrogens of PH_2. With this zero level, relative IPs of protonated porphyrin (or hydroporphyrin) nitrogens will be generally positive, corresponding to higher core IPs of the protonated porphyrin nitrogens relative to unprotonated nitrogens.[4a,10]

Since EC-based IPs are calculated in an essentially ΔSCF-type manner, our LDF-EC "IPs" account for differences in

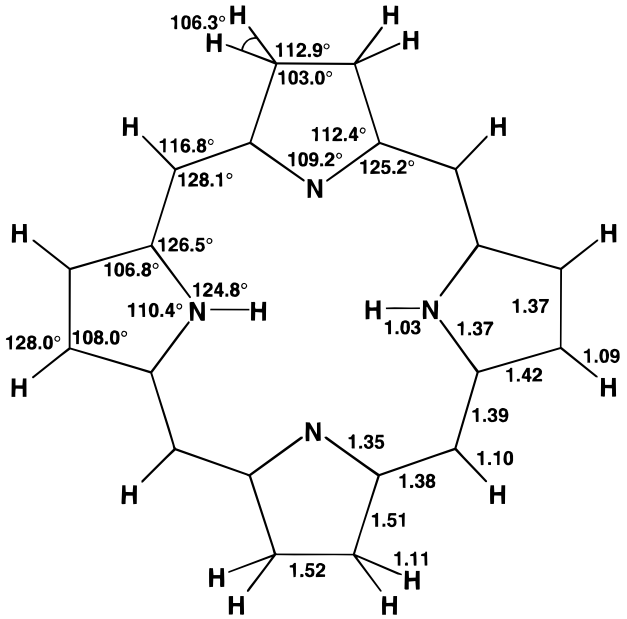

Figure 2. Symmetry-distinct internuclear distances (Å) and angles (deg) in the LDF/DNP optimized structure of BCH_2 (D_{2h}).

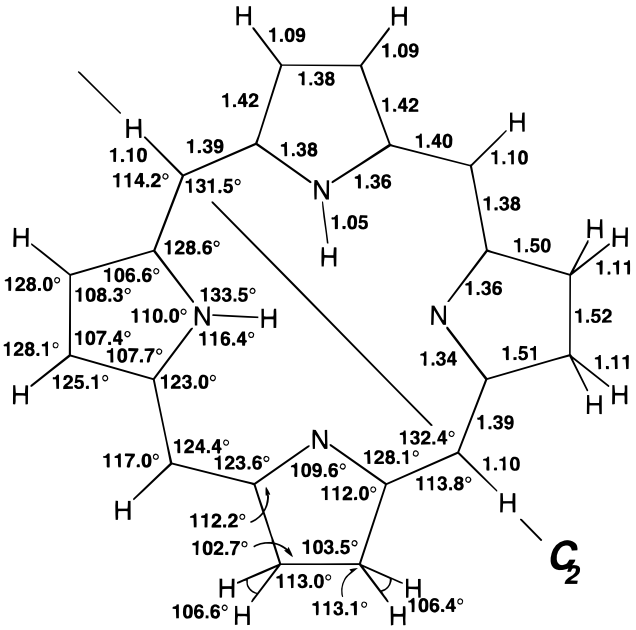

Figure 3. Symmetry-distinct internuclear distances (Å) and angles (deg) in the LDF/DNP optimized structure of *cis*-$IBCH_2$ (C_{2v}).

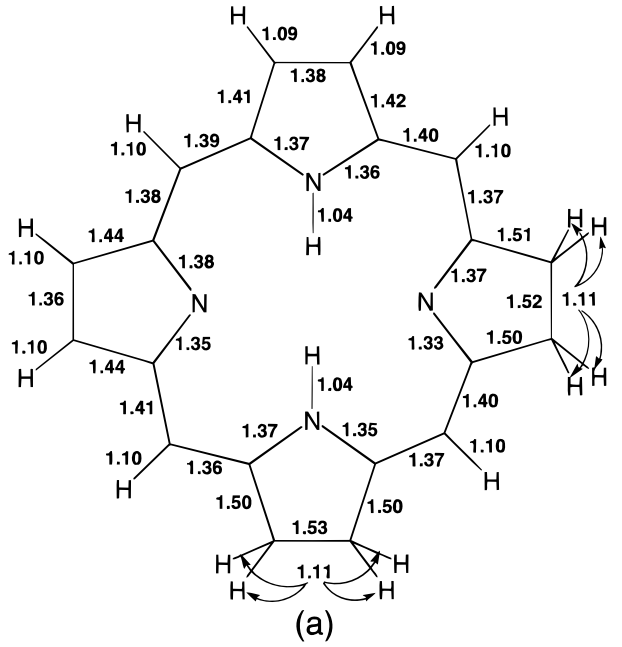

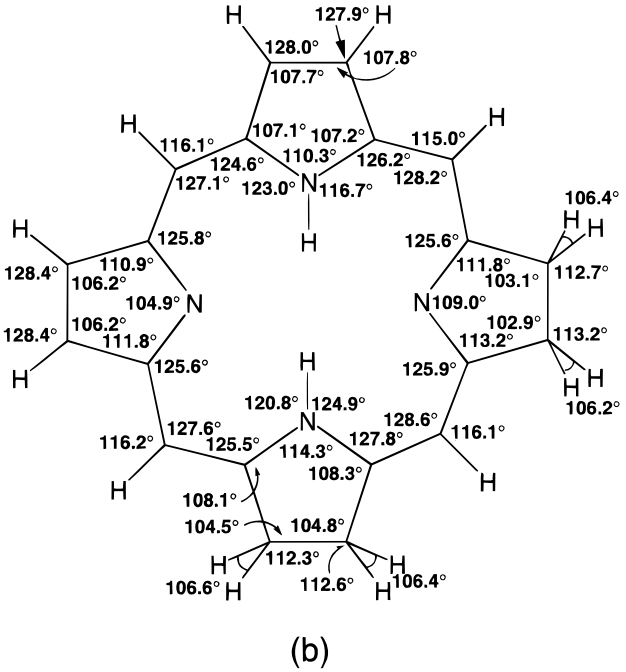

Figure 4. Symmetry-distinct internuclear (a) distances (Å) and (b) angles (deg) in the LDF/DNP optimized structure of *trans*-$IBCH_2$ (D_{2h}).

orbital relaxation energies for different molecules. Also, since our density functional includes a correlation functional, the LDF-EC "IPs" have taken some account of electron correlation effects.

III. Results and Discussion

A. Molecular Structures. The LDF/DNP optimized geometries of BCH_2, *cis*-$IBCH_2$, and *trans*-$IBCH_2$ are shown in Figures 2, 3, and 4, respectively. LDF/DNP optimized structures of PH_2 and CH_2 are not shown, since essentially the same structures, obtained with a slightly different basis set, have been published elsewhere.[3]

To put the molecular structures of hydroporphyrins[18] in perspective, a few words may be said on the molecular structures of porphyrins. In the LDF optimized structure of porphyrin,[3] the $C_\alpha-C_\beta$ bonds (ca. 1.42−1.44 Å) are the longest bonds in the macrocycle, followed by the $C_\alpha-C_{meso}$ (ca. 1.38 Å), $C_\beta-C_\beta$ (ca. 1.37 Å), and $C_\alpha-N$ (ca. 1.36 Å) bonds. Similar bond lengths are also seen in a wide variety of porphyrins, but the order of bond length for the last three types of bonds can vary. In free base porphyrins, the $C_\alpha-N-C_\alpha$ angle is significantly larger in the pyrrole rings with the protonated nitrogens (ca. 110−111°) than in the pyrrole rings with the unprotonated nitrogens (ca. 105°).[3,19] The porphyrin macrocycle readily undergoes out-of-plane distortions such as ruffling, saddling, and doming as a result of metal ion complexation, steric effects of peripheral substituents, etc.[20,21] The central $C_{12}N_4$ ring is also quite flexible with respect to in-plane deformation, as may be seen in the LDF optimized geometry of *cis*-porphyrin (an intermediate in the N−H tautomerism of free base porphyrins)[22] and the crystallographic structure of a planar thallium porphyrin.[23] The calculated structural data on hydroporphyrins allow the following generalizations and insights.

The optimized hydroporphyrin structures show that $C_\beta-C_\beta$ hydrogenation causes both the $C_\beta-C_\beta$ and $C_\alpha-C_\beta$ bonds to lengthen to typical single-bond lengths of 1.51−152 Å, with the $C_\alpha-C_\beta$ bonds (1.51 Å) being barely shorter than the $C_\beta-C_\beta$ bonds (1.52 Å).

As expected, tetrahedralization of the β carbons results in a slight compression of the $C_\alpha-C_\beta-C_\beta$ angles (103−105°), relative to those in PH_2 (106−107°). This results in a widening of the $C_\alpha-N-C_\alpha$ angle in the hydrogenated rings of hydroporphyrins relative to porphyrins. Thus, in all of the optimized hydroporphyrin structures, the $C_\alpha-N-C_\alpha$ angles in the hydrogenated N-unprotonated rings are each 109−110°, which may be compared to a value of 105° for the $C_\alpha-N-C_\alpha$ angle in N-unprotonated pyrrole rings in porphyrin. Thus, the $C_\alpha-N-C_\alpha$ angle widens as a result of both N-protonation[19] and $C_\beta-C_\beta$ hydrogenation of the pyrrole ring in question.[18]

The role of these two factors (N-protonation and $C_\beta-C_\beta$ hydrogenation) can be clearly seen in the optimized structure of *trans*-$IBCH_2$. Thus, in the N-protonated, $C_\beta-C_\beta$ hydrogenated pyrrole ring, the $C_\alpha-N-C_\alpha$ angle is largest (114.3°). In the N-protonated unhydrogenated pyrrole ring and the N-unprotonated $C_\beta-C_\beta$ hydrogenated pyrrole ring, the $C_\alpha-N-C_\alpha$ angle is of an intermediate magnitude (109−110°), which is about the same as the $C_\alpha-N-C_\alpha$ angles in the N-protonated rings of PH_2. In the ring that is neither hydrogenated nor N-protonated, the $C_\alpha-N-C_\alpha$ angle is smallest at 104.9°, essentially the same as that in an N-unprotonated ring of PH_2.

In crystallographic studies of metallohydroporphyrins, the widened $C_\alpha-N-C_\alpha$ angle in a hydrogenated ring of a hydroporphyrin is known to slightly affect the metal−nitrogen distance involving the reduced ring. Thus, the metal−nitrogen distances involving the hydrogenated rings lengthen relative to a porphyrin, provided the hydroporphyrin and the porphyrin being compared have the "same" conformation.[17] The effect has been best seen in a crystal structure of zinc tetraphenylbacteriochlorin, where the Zn−N distances average 2.12 and 2.04 Å for the reduced and unreduced rings, respectively. Other similar examples are known.[17] Our calculated free base structures show an analogous structural trend. The distances between the protonated nitrogens in PH_2, CH_2, and BCH_2 are 4.18, 4.17, and 4.14 Å, i.e., varying within the small range 4.16 ± 0.02 Å. In contrast, the distances between the unprotonated nitrogens in PH_2, CH_2, and BCH_2 are 4.04, 4.12, and 4.24 Å, increasing dramatically with $C_\beta-C_\beta$ hydrogenation. In other words, hydrogenation of a pyrrole ring results in the nitrogen atom moving away from the porphyrin center (definable, e.g., as the centroid of the four tetrapyrrole nitrogens).

The structure of *cis*-$IBCH_2$ exhibits clear evidence of repulsion between the two central hydrogens and is reminiscent of LDF optimized geometry of *cis*-porphyrin, published elsewhere.[22,24] The N−H bonds are directed such that they are far from bisecting the $C_\alpha-N-C_\alpha$ angles. Thus, at each imino nitrogen, the two $C_\alpha-N-H_{imino}$ angles are widely different, 116.4 and 133.5°. Another manifestation of this repulsion is a remarkable, experimentally unprecedented distortion of the central $C_{12}N_4$ ring, which is shortened along the molecular C_2 axis and lengthened in a direction perpendicular to it. Thus, the $C_\alpha-C_{meso}-C_\alpha$ angles, which are bisected by the molecular C_2 axis, are about 7° wider than the other $C_\alpha-C_{meso}-C_\alpha$ angles. Similarly, the four $N-C_\alpha-C_{meso}$ angles closest to the C_2 axis are about 5° wider than the other $N-C_\alpha-C_{meso}$ angles. Compared to PH_2, the central N_4 core of *cis*-$IBCH_2$ has a pronounced rectangular shape. Thus, the two protonated central nitrogens are 3.21 Å apart, and the two unprotonated nitrogens are 3.20 Å apart. In contrast, the distance between a protonated nitrogen and its nearest unprotonated nitrogen is only 2.71 Å. For comparison, the distance between nearest-neighbor nitrogens in PH_2 is 2.91 Å.

As mentioned above, single-point RHF/DZ and RMP2/DZ calculations were performed on the LDF optimized geometries of the *cis* and *trans* tautomers of $IBCH_2$. At the LDF, HF, and MP2 levels, the energy of the *cis* isomer was found to be −3.45, 2.38, and 1.74 kcal/mol relative to the *trans* isomer chosen as the zero level. In other words, our calculations indicate that the two tautomers are of essentially equal energy. This is in accord with the simultaneous spectroscopic detection of both *cis* and *trans* tautomers for unsubstituted isobacteriochlorin[25] and for an alkyl-substituted isobacteriochlorin.[26]

Finally, the LDF optimized geometry of *trans*-$IBCH_2$ provides a good illustration of the advantage of density functional theory over Hartree−Fock theory in geometry optimization studies of tetrapyrroles.[3] *trans*-$IBCH_2$ has only C_s symmetry, and no symmetry constraint can force an averaging of its two nonzwitterionic resonance forms.

B. Valence Ionization Potentials. The HF-KT and LDF IPs of PH_2 have been discussed in detail elsewhere.[4a,b] A database of HF-KT and LDF valence IPs is also available for a variety of substituted porphyrins.[12] The main conclusions from these investigations, as far as they are relevant to this study, are as follows.

Hartree−Fock and density functional theories have played complementary roles in our theoretical analyses of photoelectron spectra.[10,12,14] The advantage of HF theory is that it provides a broad view of all one-electron IPs, both core and valence, of a molecule. In contrast, although DFT orbital energies often exhibit patterns that are qualitatively similar to their HF counterparts, the former cannot be identified with IPs via Koopman's theorem. In quantitative terms, DFT orbital energies are in much poorer agreement with photoelectron spectra than HF-KT IPs. This is the reason why we only use ΔSCF-type DFT calculations to calculate valence IPs. The disadvantage of DFT in this regard is that it is applicable only to the lowest-energy state of each symmetry. Thus, our set of calculated LDF IPs is necessarily very incomplete.

The HF orbital energy spectrum can qualitatively reproduce the peak clustering pattern in the UPS of PH_2 in the regime IP < 13 eV.[4a] However, for well-understood reasons (neglect of relaxation and correlation effects, etc.),[4b,12] the absolute values of certain HF-KT valence IPs in the 0−13 eV regime deviate from experimental values by as much as 0.5−1.0 eV. Errors of this magnitude imply that HF theory, while useful, can be inadequate for accurate analyses of photoelectron spectra. In contrast, the absolute values of LDF IPs of porphyrins are generally in excellent agreement with gas-phase UPS, with discrepancies between calculation and experiment being only about 0.0−0.3 eV.[4b,12] Improvements in the quality of the density functionals and basis sets employed should result in even closer agreement between theory and experiment.

Table 1 presents the HF-KT IPs corresponding to the nine highest occupied MOs of each of the tetrapyrroles studied in this work. Table 2 presents one to three LDF valence IPs for each molecule, depending on the molecular symmetry (see Methods section). The following points merit discussion with regard to these results.

As one may qualitatively expect from the four-orbital model, the two lowest IPs of all the molecules are well-separated energetically from other IPs. This not only is valid at the Hartree−Fock level but also can be seen in the LDF results for PH_2, BCH_2, and *cis*-$IBCH_2$.

TABLE 1: HF-KT (HF/DZ//LDF/DNP) Valence IPs (eV) of PH_2, CH_2, BCH_2, and *cis*- and *trans*-$IBCH_2$

			$IBCH_2$	
PH_2	CH_2	BCH_2	*cis*	*trans*
6.36 (b_{1u})	5.93 (a_2)	5.23 (a_u)	5.71 (a_2)	5.65 (a'')
6.36 (a_u)	6.54 (b_2)	6.38 (b_{1u})	6.57 (b_2)	6.97 (a'')
9.00 (b_{2g})	8.73 (b_2)	9.29 (b_{2g})	9.37 (b_2)	8.49 (a'')
9.20 (b_{1u})	9.68 (a_2)	9.83 (b_{3g})	9.61 (a_2)	9.47 (a'')
10.12 (b_{3g})	10.07 (a_2)	9.86 (b_{2g})	9.76 (a_2)	9.61 (a'')
10.20 (b_{3g})	10.08 (b_2)	9.87 (b_{1u})	9.82 (b_2)	9.66 (a'')
10.21 (b_{1u})	10.16 (b_2)	11.17 (a_g)	10.59 (b_1)	10.79 (a')
10.43 (b_{2g})	11.07 (a_1)	11.28 (b_{2u})	11.23 (a_1)	11.18 (a')
11.18 (a_g)	11.23 (a_1)	11.40 (a_u)	11.52 (b_2)	11.31 (a'')

TABLE 2: LDF (LDF/DNP//LDF/DNP) Valence IPs (eV) of PH_2, CH_2, BCH_2, and *cis*- and *trans*-$IBCH_2$

				$IBCH_2$	
IP	PH_2	CH_2	BCH_2	*cis*	*trans*
IP_1	7.23 (B_{1u})	6.92 (A_2)	6.42 (A_u)	6.52 (A_2)	6.42 (A'')
IP_2	7.44 (A_u)	7.11 (B_2)	6.99 (B_{1u})	6.95 (B_2)	
IP_3	8.24 (B_{2g})		8.14 (B_{2g})	8.43 (B_1)?	

At the Hartree−Fock level, while the a_u and b_{1u} HOMOs of PH_2 have the same orbital energy, the HOMOs of all the hydroporphyrins studied are clearly of the a_{1u}-type (spin densities of the lowest cation radical states are discussed in the next section). At the LDF level, the lowest vertical IP of PH_2 corresponds to a $^2B_{1u}$ (i.e., A_{2u}-type) cation radical state, with the next lowest cation state (^2A_u) 0.2 eV higher. As at the HF level, the lowest vertical LDF IPs of all the hydroporphyrins correspond to A_{1u}-type cation radical states. This is in accord with the experimental observation that all hydroporphyrin cation radicals are of the A_{1u}-type.[2b,27,28]

The reason for the universal A_{1u}-type character of hydroporphyrin cation radicals can be qualitatively understood as follows. The a_u (a_{1u}-type) and b_{1u} (a_{2u}-type) HOMOs of PH_2 have small-but-significant and zero amplitudes at the β positions, respectively. Thus, one would expect that $C_\beta-C_\beta$ hydrogenation should primarily destabilize the a_{1u}-type porphyrin HOMO and affect the a_{2u}-type HOMO in only a secondary manner. Both the HF-KT and LDF IPs support the essential validity of this expectation.

We now examine the influence of macrocycle hydrogenation in more quantitative terms. Dihydrogenation of PH_2 lowers the lowest IP by 0.43 eV at the HF level and by 0.41 eV at the LDF level. Dihydrogenation of chlorin to give bacteriochlorin lowers the lowest IP by 0.71 eV at the HF level and by 0.5 eV at the LDF level. BCH_2 and the two tautomers of $IBCH_2$ have about the same lowest IPs at the LDF level, but at the HF level, the lowest IP of BCH_2 is significantly lower than that of either tautomer of $IBCH_2$. Another significant difference between the HF and LDF results is concerned with the energy gap between the lowest and second lowest IPs of hydroporphyrins. Note that this gap is large for CH_2 and *cis*-$IBCH_2$ (0.61 and 0.86 eV, respectively) and very large for BCH_2 and *trans*-$IBCH_2$ (1.15 and 1.32 eV, respectively). At the LDF level, these gaps are much more moderate, ranging from 0.2 to 0.5 eV for the various compounds examined. Thus, the LDF results suggest that the four-orbital model of porphyrin electronic structure applies reasonably well to hydroporphyrin IPs and photoelectron spectra.

On the whole, although the absolute values of the HF-KT and LDF valence IPs are rather different (sometimes by over 1 eV, as in the case of the first IP of BCH_2), the two theories agree much better for shifts in IPs due to macrocycle hydrogenation. However, where the two theories predict significantly different electronic effects due to hydrogenation, the LDF results are considered to be much more reliable on the basis of considerable previous experience.[4b,12] Indeed, for all the parent hydroporphyrins studied in this investigation, for which no UPS data are available, the absolute values of the LDF IPs are expected to be within 0.0−0.3 eV of the true IPs. Thus, our collection of LDF results (Table 2) serves as a good, albeit incomplete, substitute for the much-needed experimental photoelectron spectra.

Stolzenberg *et al*. have reported macrocycle-centered oxidation potentials for a number of different metal complexes of octaethylporphyrin, octaethylchlorin, and octaethylisobacteriochlorin.[29] In each step (for every dihydrogenation), the oxidation potential was found to diminish by approximately 300 mV. Chang *et al*. have reported macrocycle-centered oxidation potentials for free base and zinc tetraphenylhydroporphyrins.[30] Compared to Stolzenberg *et al*., the latter authors found a somewhat smaller difference (<200 mV) in oxidation potential between the porphyrin and chlorin ring systems.[30] In the tetraphenyl series, the oxidation potentials of bacteriochlorins and isobacteriochlorins were found to be less than those of the chlorins by 300−500 mV. Overall, these electrochemical results are in good agreement with our calculated trends in valence IPs at the LDF level.

C. Atomic Spin Populations in Cation Radicals. Figure 5 depicts LDF atomic spin populations of the lowest cation radical states of the different compounds studied. For the A_{1u}-type radicals, unpaired spin density is localized largely on the α carbons and slightly on the β carbons, with negligible amounts elsewhere. For the A_{2u}-type radicals, unpaired spin density is concentrated on the *meso* carbons and the nitrogens, with negligible amounts elsewhere. In the hydroporphyrins, the tetrahedral carbons don't carry any significant spin population. The slight negative spin populations correspond to minority spin and stem from the spin-unrestricted nature of the open-shell calculations. Concerning Figure 5, the most notable point appears to be the extreme similarity in the pattern of spin density distribution in the various compounds. Even in PH_2, the β carbons carry significant but quite small spin populations. Accordingly, it is not surprising that $C_\beta-C_\beta$ hydrogenation brings about only modest changes in the overall pattern of spin density distribution. The isobacteriochlorin radicals exhibit the greatest deviation from the porphyrin-type spin distribution. Thus, there is a small but significant spin population on the *meso* carbon bridging the unhydrogenated N-protonated pyrrole ring and the hydrogenated N-unprotonated pyrrole ring in the A_{1u} cation radicals of both tautomers of $IBCH_2$.

D. Core Ionization Potentials. Nitrogen core IPs of a wide range of porphyrins have been studied both experimentally by XPS[10,14,31,32] and theoretically by *ab initio* HF calculations.[10,14] Both methods have shown that these core IPs are excellent sensors of substituent electronic effects in porphyrins. In contrast to the extensive work on porphyrins, there has been only one serious investigation of nitrogen core IPs of hydroporphyrins.[33] We have repeated the XPS measurements reported in this work and, except for a uniform shift in the absolute values of the binding energies, our results confirm all the trends observed by the earlier workers. However, armed with high-quality calculated results, we achieve here a better interpretation of the XPS results relative to the earlier workers. Tables 3 and 4 present HF-KT and LDF-EC relative nitrogen core IPs for the different compounds studied. Table 5 presents our nitrogen core XPS remeasurements for $TPPH_2$, $TPCH_2$, and $TPBCH_2$, along with LDF-EC results for $TPPH_2$ and $TPBCH_2$.

Before proceeding further, it is advantageous to present a shorthand description of the different types of nitrogen in our molecules of interest. In PH_2, BCH_2, and *cis*-$IBCH_2$, there are

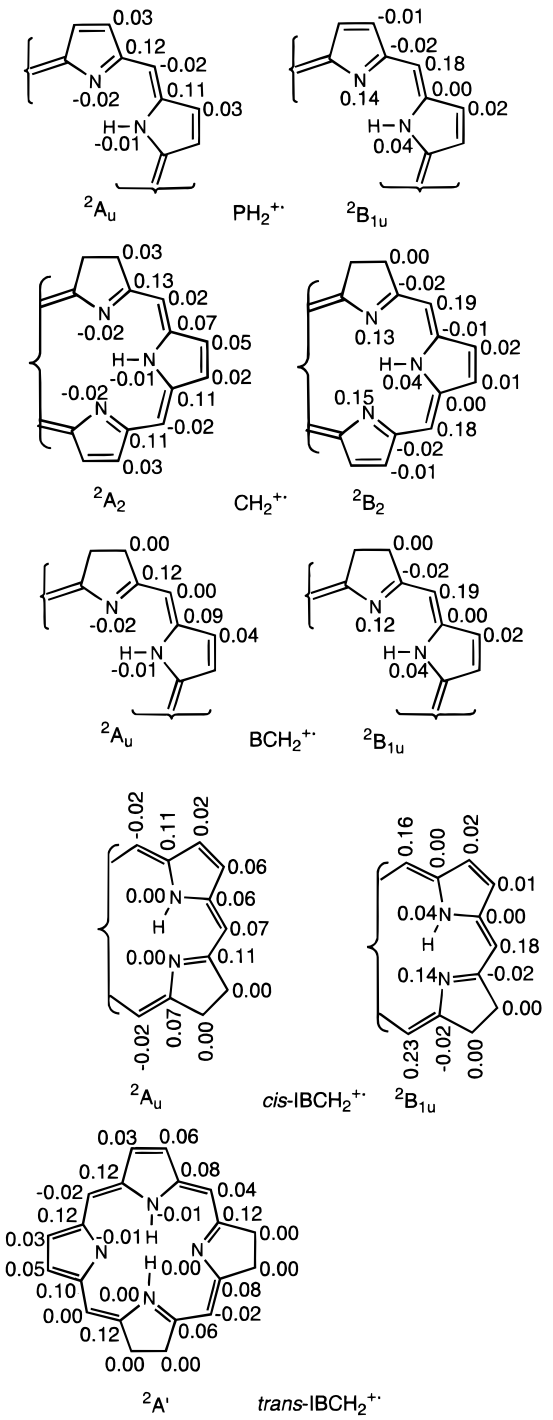

Figure 5. LDF spin populations of non-hydrogen atoms in tetrapyrrole cation radicals. Results for A_{1u}- and A_{2u}-type radicals are given in the left and right columns, respectively.

only two types of nitrogen, protonated (N_p) and unprotonated (N_u). In CH_2, there are two types of N_u, one in the hydrogenated ring (N_{u1}) and one opposite to it (N_{u2}). In *trans*-$IBCH_2$, the protonated nitrogens in the hydrogenated and unhydrogenated pyrrole rings are named N_{p1} and N_{p2} and the unprotonated nitrogens in the hydrogenated and unhydrogenated pyrrole rings are named N_{u1} and N_{u2}. The symbol ΔE_{p-u} will be used to refer to the energy difference between the (mean) core IPs of the protonated and unprotonated nitrogens.

Both HF and LDF theories predict that in each molecule the protonated nitrogens have higher core IPs than the unprotonated nitrogens.[4a,10] The calculated values of ΔE_{p-u} of PH_2 are 1.82 and 2.36 eV at the HF-KT and LDF-EC levels, respectively.

TABLE 3: HF-KT Nitrogen Core IPs (eV) Relative to N_{u1} of PH_2 as Zero Level

				$IBCH_2$	
N	PH_2	CH_2	BCH_2	*cis*	*trans*
unprotonated					
N_{u1}	**0.00**	0.20	0.91	0.32	−0.17
N_{u2}		0.69			0.67
protonated					
N_{p1}	1.82	1.83	1.71	1.66	1.61
N_{p2}					2.29
ΔE_{p-u}	1.82	1.39	0.8	1.34	1.70

TABLE 4: LDF-EC Core IPs (eV) Relative to N_p of PH_2 as Zero Level

				$IBCH_2$	
N	PH_2	CH_2	BCH_2	*cis*	*trans*
unprotonated					
N_{u1}	**0.00**	−0.14	0.27	0.18	−0.36
N_{u2}		0.41			0.38
protonated					
N_{p1}	2.36	2.22	2.11	1.98	1.57
N_{p2}					1.97
ΔE_{p-u}	2.36	2.10	1.84	1.80	1.76

TABLE 5: LDF-EC and XPS Core IPs of $TPPH_2$, $TPCH_2$, and $TPBCH_2$ Relative to N_u of PH_2

	PH_2		$TPPH_2$		$TPCH_2$	$TPBCH_2$	
N	LDF	XPS	LDF	XPS	XPS	LDF	XPS
N_u	**0.00**	0.0	−0.30	−0.6	−0.25	0.00	−0.05
N_p	2.36	2.1	1.99	1.5	1.65	1.85	1.75
ΔE_{p-u}	2.36	2.1	2.29	2.1	1.9	1.85	1.8

Experimentally, this energy difference is 2.1 eV,[4a] which represents reasonably good agreement between theory and experiment for either calculational method. The two calculational methods also predict a core IP difference of about 0.5 eV between the two symmetry-distinct unprotonated nitrogens of CH_2, which agrees with the observation of an unresolved XPS peak for the unprotonated nitrogens of $TPCH_2$. From the calculations, we know that the unprotonated nitrogen in the hydrogenated pyrrole ring has a higher core IP relative to the other unprotonated nitrogen in the unhydrogenated pyrrole ring.

Both the HF (Table 3) and LDF (Table 4) results show that hydrogenation of a pyrrole ring is accompanied by a significant increase in the core IP of the nitrogen in the same ring and smaller changes in nitrogen core IPs for the other rings. This has the consequence that ΔE_{p-u} shrinks as one progresses from PH_2 through CH_2 to BCH_2 or $IBCH_2$. The XPS results on *meso*-tetraphenyl tetrapyrroles (Table 5) qualitatively confirm these calculated trends.[32] Thus, as far as nitrogen core IPs or nitrogen electrostatic potentials are concerned, a hydrogenated $C_\beta-C_\beta$ linkage behaves as a mildly electron-withdrawing group relative to an unreduced $C_\beta-C_\beta$ linkage.

A more detailed examination of results of Tables 3−5 shows several discrepancies between HF-KT, LDF-EC, and XPS results.

Although HF theory gives a reasonably good value for ΔE_{p-u} for PH_2, the analogous values for CH_2 (1.39 eV) and BCH_2 (0.8 eV) compare rather unfavorably with experimental XPS values of $TPCH_2$ (1.9 eV) and $TPBCH_2$ (1.8 eV),[32] which imply errors of approximately 0.5 and 1.0 eV, respectively (Table 5). Errors of this magnitude are unacceptable, since they imply that our HF/DZ//LDF/DNP calculations probably cannot predict some of the more detailed features of the nitrogen XPS of nonprototype hydroporphyrins.

The failure of our HF/DZ//LDF/DNP calculations to provide reasonable values for ΔE_{p-u}s of hydroporphyrins is somewhat

surprising. In older work, HF/DZ calculations have provided excellent simulations of the nitrogen core XPS of PH_2,[4a] a series of tetraphenylporphyrins,[10] and tetraazaporphyrins.[14] In view of our extensive studies of basis set effects for tetrapyrroles,[4a,10] we believe that the error in this case does not arise from an inadequate basis set at the HF level. We considered the possibility that this error might have resulted from bad molecular geometries. LDF geometry optimizations of BCH_2 with progressively lower symmetry constraints gave structures very close to the optimized D_{2h} symmetry-constrained structure. HF calculations on the new structures failed to provide a realistic ΔE_{p-u} for BCH_2. Finally, having ruled out a variety of other possibilities, we considered it likely that HF theory provides a poor description of the molecular charge distributions of hydroporphyrins. This led us to perform the LDF-EC calculations. While numerous equivalent-core calculations have been performed at the Hartree−Fock level,[34] we believe that this work provides the first examples of equivalent-core calculations with density functional theory.

The LDF-EC values of the ΔE_{p-u} of CH_2 and BCH_2 are 2.10 and 1.84 eV, respectively, which agree quite favorably with the XPS values of 1.9 and 1.8 eV for $TPCH_2$ and $TPBCH_2$, respectively. Thus, the flawed charge distribution at the HF level is largely corrected at the LDF level, i.e., with the use of a modest treatment of electron correlation. Note from the results on $TPPH_2$ and $TPBCH_2$ in Table 5 that LDF theory provides a reasonable description the electron-withdrawing influence of $C_\beta-C_\beta$ hydrogenation on N_u. However, whereas the N_p core IP of $TPBCH_2$ is higher than that of $TPPH_2$ by 0.25 eV, LDF theory predicts that the former is lower than the latter by 0.14 eV. Finally, the ΔE_{p-u} of both the *cis* and *trans* tautomers of $IBCH_2$ are nearly equal, 1.78 ± 0.02 eV. XPS experiments are planned to confirm the calculated features of the molecular charge distributions of isobacteriochlorins.

Overall, in spite of slight imperfections, the LDF-EC method is far more accurate than *ab initio* Hartree−Fock theory for analyzing XPS spectra of tetrapyrroles. There is little doubt that correlated *ab initio* methods such as MP2 could have been used in conjunction with the EC approximation to achieve the same performance, but this would have involved rather higher computational cost. We plan to examine the performance of the EC approximation at a variety of correlated levels in a future study. For now, we only point out that the EC approximation used in conjunction with DFT should be a convenient and reliable aid to XPS-based chemical state analysis of a wide variety of materials.

IV. Summary and Conclusions

The principal conclusions of this work can be enumerated as follows.

(1) For structural studies of hydroporphyrins, as for many other classes of molecules of similar size, DFT appears to be the method of choice. Thus, the LDF optimized geometries provide a detailed and accurate picture of the structural effects of peripheral hydrogenation on the $C_\alpha-C_\beta$ and $C_\beta-C_\beta$ bond distances, the $C_\alpha-C_\beta-C_\beta$ and $C_\alpha-N-C_\alpha$ angles, and the size of the central metal-binding cavity of the macrocycles.

(2) Steric repulsion between the central hydrogens of *cis*-$IBCH_2$ results in a unique elongation of the central $C_{12}N_4$ macrocycle. The structure is reminiscent of the LDF optimized geometry of *cis*-porphyrin, an intermediate in the double-proton migration of free base porphyrins, but is otherwise unprecedented in the structural chemistry of tetrapyrroles.

(3) Some of the lower valence IPs of various parent tetrapyrroles have been calculated by LDF ΔSCF calculations. The notable feature of these IPs is that their absolute values are expected to be extremely accurate, with maximum errors of only 0.3 eV relative to true experimental values. This stands in sharp contrast to errors of as much as 1 eV or more in HF-KT or HF-ΔSCF IPs. It follows that the LDF ΔSCF IPs also provide a very accurate picture of the electronic differences among the different tetrapyrroles studied.

(4) LDF equivalent-core calculations provide accurate simulations of the nitrogen core XPS of hydroporphyrins. This indicates that DFT gives a good description of the molecular charge distributions of hydroporphyrins. Relative to the LDF-EC results, nitrogen core IP patterns obtained from HF calculations are in much poorer agreement with XPS data.

(5) Overall, DFT emerges as a versatile and accurate tool for theoretical studies of tetrapyrroles. In contrast, HF theory, already known to be unsuitable for structural studies of tetrapyrroles, provides a significantly less accurate description of the electronic properties of hydroporphyrins. Correlated *ab initio* calculations on tetrapyrroles, currently rather expensive, remain an important goal for the future.

Acknowledgment. This work was supported by the Research Council of Norway and a Senior Fellowship of the San Diego Supercomputer Center.

References and Notes

(1) (a) Scheer, H. In *Chlorophylls*; Scheer, H., Ed.; CRC Press: Boca Raton, FL, 1991; pp 3−30. (b) Montfors, F. P.; Gerlach, B.; Höper, F. *Chem. Rev.* **1994**, *94*, 327.

(2) (a) Hanson, L. S. In *Chlorophylls*; Scheer, H., Ed.; CRC Press: Boca Raton, FL, 1991; pp 993−1014. (b) Plato, M.; Möbius, K.; Lubitz, W. In *Chlorophylls*; Scheer, H., Ed.; CRC Press: Boca Raton, FL, 1991; pp 1015−1046.

(3) Almlöf, J.; Fischer, T. H.; Gassman, P. G.; Ghosh, A.; Häser, M. *J. Phys. Chem.* **1993**, *97*, 10964.

(4) First-principles calculations on porphyrin: (a) Ghosh, A.; Almlöf, J.; Gassman, P. G. *Chem. Phys. Lett.* **1991**, *186*, 113. (b) Ghosh, A.; Almlöf, J. *Chem. Phys. Lett.* **1993**, *213*, 519. (c) Merchan, M.; Orti, E.; Roos, B. O. *Chem. Phys. Lett.* **1994**, *226*, 27.

(5) For additional examples of geometry optimizations at this level of theory and comparisons with experiment, see: (a) Ghosh, A.; Almlöf, J.; Que, L., Jr. *J. Phys. Chem.* **1994**, *98*, 5576. (b) Ghosh, A. *Angew. Chem., Int. Ed. Engl.* **1995**, *34*, 1028; *Angew. Chem.* **1995**, *107*, 1117. (c) Kalsbeck, W. A.; Ghosh, A.; Pandey, R. K.; Smith, K. M.; Bocian, D. F. *J. Am. Chem. Soc.* **1995**, *117*, 10959. (d) Ghosh, A.; Almlöf, J.; Que, L., Jr. *Angew. Chem., Int. Ed. Engl.* **1996**, *35*, 770; *Angew. Chem.* **1996**, *108*, 846. (e) Ghosh, A.; Bocian, D. F. *J. Phys. Chem.* **1996**, *100*, 6363. (f) Vangberg, T.; Ghosh, A. *J. Phys. Chem. B* **1997**, *101*, 1496.

(6) von Barth, U.; Hedin, L. *J. Phys. C* **1972**, *5*, 1629.

(7) (a) The DMol program can be obtained from: Molecular Simulations, Inc., 9685 Scranton Road, San Diego, CA 92121-2777. (b) Delley, B. *J. Chem. Phys.* **1990**, *92*, 508.

(8) The DZ basis sets were obtained from: van Duijneveldt, F. B. IBM Research Report RJ945, 1971. The basis sets were (6s3p)/[3s2p] for C and N (3s)/[2s] for H, with the outermost s and p primitives uncontracted and allowed to act as basis functions by themselves.

(9) (a) Almlöf, J.; Faegri, K.; Feyereisen, M. W.; Korsell, K. DISCO, a direct SCF and MP2 code. (b) Almlöf, J.; Faegri, K.; Korsell, K. *J. Comput. Chem.* **1982**, *3*, 385.

(10) Gassman, P. G.; Ghosh, A.; Almlöf, J. *J. Am. Chem. Soc.* **1992**, *114*, 9990.

(11) Ghosh, A.; Gassman, P. G.; Almlöf, J. *J. Am. Chem. Soc.* **1994**, *116*, 1932.

(12) (a) For extensive LDF ΔSCF calculations of valence IPs of porphyrins, see: Ghosh, A. *J. Am. Chem. Soc.* **1995**, *117*, 4691. (b) For nonlocal DFT calculations of porphyrin valence IPs, see: Ghosh, A.; Vangberg, T. *Theor. Chim. Acta* (Jan Almlöf memorial issue), in press.

(13) For a recent LDF study of valence IPs of tetraphenylporphyrins, see: Ghosh, A. *J. Mol. Struct.: THEOCHEM* **1996**, *388*, 359.

(14) Ghosh, A.; Fitzgerald, J.; Gassman, P. G.; Almlöf, J. *Inorg. Chem.* **1994**, *33*, 6057.

(15) Ghosh, A. *J. Phys. Chem.* **1994**, *98*, 11004.

(16) Jolly, W. L.; Hendrickson, D. N. *J. Am. Chem. Soc.* **1970**, *92*, 1863.

(17) Hollander, J. M.; Jolly, W. L. *Acc. Chem. Res.* **1970**, *3*, 193.

(18) Barkigia, K. M.; Fajer, J. In *The Photosynthetic Reaction Center*; Deisenhofer, J., Norris, J. R., Eds.; Academic Press: San Diego, CA, 1993; Vol. 2, p 513.

(19) Hoard, J. L. In *Porphyrin and Metalloporphyrins*; Smith, K. M., Ed.; Elsevier: Amsterdam, 1975; p 317.

(20) Scheidt, W. R.; Lee, Y. J. *Struct. Bonding* **1987**, *64*, 1.

(21) Ravikanth, M.; Chandrashekhar, T. K. *Struct. Bonding* **1995**, *82*, 105.

(22) Ghosh, A.; Almlöf, J. *J. Phys. Chem.* **1995**, *99*, 11004.

(23) Senge, M. O. *J. Chem. Soc., Dalton Trans.* **1993**, 3539.

(24) To our knowledge, there is only one example of a crystal structure of a *cis*-porphyrinic molecule, viz. a free base dioxoisobacteriochlorin: Barkigia, K. M.; Chang, C. K.; Fajer, J.; Renner, M. W. *J. Am. Chem. Soc.* **1992**, *114*, 1701. However, the poor quality of the structure has apparently precluded a detailed geometrical analysis of the *cis*-porphyrinic molecular framework.

(25) Huang, W. Y.; Wild, U. P.; Johnson, L. W. *J. Phys. Chem.* **1992**, *96*, 6189.

(26) Chang, C. K. *Biochemistry* **1980**, *19*, 1971.

(27) Ozawa, S.; Watanabe, Y.; Morishima, I. *J. Am. Chem. Soc.* **1994**, *116*, 5832.

(28) Richardson, P. E.; Chang, C. K.; Spaulding, L. D., Fajer, J. *J. Am. Chem. Soc.* **1979**, *101*, 7736.

(29) (a) Stolzenberg, A. M.; Strauss, S. H.; Holm, R. H. *J. Am. Chem. Soc.* **1981**, *103*, 4763. (b) Stolzenberg, A. M.; Schussel, L. J. *Inorg. Chem.* **1991**, *30*, 3205.

(30) Chang, C. K.; Hanson, L. K.; Richardson, P. F.; Young, R.; Fajer, J. *Proc. Natl. Acad. Sci. U.S.A.* **1981**, *78*, 2652.

(31) Ghosh, A. *J. Org. Chem.* **1993**, *58*, 6932.

(32) Goll, J. G.; Moore, K. T.; Ghosh, A.; Therien, M. J. *J. Am. Chem. Soc.* **1996**, *118*, 8344−8354.

(33) Karweik, D. H.; Winograd, N. *Inorg. Chem.* **1976**, *15*, 2336.

(34) See, for example: Adams, D. B. *J. Electron Spectrosc. Relat. Phenom.* **1993**, *61*, 241 and references therein.